

# On $\gamma_5$ schemes and the interplay of SMEFT operators in the Higgs-gluon coupling

Stefano Di Noi,<sup>1,\*</sup> Ramona Gröber,<sup>1,†</sup> Gudrun Heinrich,<sup>2,‡</sup> Jannis Lang,<sup>2,§</sup> and Marco Vitti<sup>1,3,4,¶</sup>

<sup>1</sup>*Dipartimento di Fisica e Astronomia “G. Galilei”, Università di Padova, Italy,  
and Istituto Nazionale di Fisica Nucleare, Sezione di Padova, I-35131 Padova, Italy*

<sup>2</sup>*Institute for Theoretical Physics, Karlsruhe Institute of Technology (KIT), D-76131 Karlsruhe, Germany*

<sup>3</sup>*Institute for Theoretical Particle Physics, Karlsruhe Institute of Technology (KIT), D-76131 Karlsruhe, Germany*

<sup>4</sup>*Institute for Astroparticle Physics, Karlsruhe Institute of Technology (KIT), D-76344 Eggenstein-Leopoldshafen, Germany*

(Dated: November 13, 2023)

We calculate the four-top quark operator contributions to Higgs production via gluon fusion in the Standard Model Effective Field Theory. The four-top operators enter for the first time via two-loop diagrams. Due to their chiral structure they contain  $\gamma_5$ , so special care needs to be taken when using dimensional regularisation for the loop integrals. We use two different schemes for the continuation of  $\gamma_5$  to  $D$  space-time dimensions in our calculations and present a mapping for the parameters in the two schemes. This generically leads to an interplay of different operators, such as four-top operators, chromomagnetic operators or Yukawa-type operators at the loop level. We validate our results by examples of matching onto UV models.

## I. INTRODUCTION

With the increasing precision in the measurement of the Higgs boson couplings, the Higgs sector has become a probe of physics beyond the Standard Model (SM). In the absence of a clear signal of new physics, potential deviations from the SM can be described as model-independently as possible by means of an effective field theory (EFT). Under the assumption that the Higgs field transforms as an  $SU(2)_L$  doublet as in the SM, heavy new physics can be described by the SM effective field theory (SMEFT) [1, 2]. In this theory, new physics effects are described by higher-dimensional operators suppressed by some large mass scale  $\Lambda$ .

In this paper we consider a subset of the possible dimension-six operators, namely the four-top quark operators, and comment on their connection to other SMEFT operators. Four-top operators are generically difficult to probe experimentally, as direct probes require the production of four top quarks. Limited by the large phase space required, four-top quark production remains a rather rare process, with a SM cross section of only about 12 fb including next-to-leading (NLO) QCD and NLO electroweak (EW) corrections for  $\sqrt{s} = 13$  TeV [3–5]. Current limits on four-top operators are hence typically rather weak, in particular mostly stemming from  $\mathcal{O}(1/\Lambda^4)$  contributions in the matrix element squared [6, 7]. For this very reason, potentially better bounds on the four-top operators can be obtained indirectly, hence by considering loop effects on other observables.

Furthermore, Ref. [8] showed that in the presence of four-top operators possible limits on the trilinear Higgs

self-coupling derived from electroweak corrections to single Higgs production [9–15] can become more restrictive. First efforts to constrain the trilinear Higgs self-coupling via single Higgs production have already been started by the experimental collaborations [16, 17].

We are going to reconsider the  $gg \rightarrow h$  computation from Ref. [8], which included effects from four-top operators within the SMEFT, using two different schemes for the continuation of  $\gamma_5$  to  $D = 4 - 2\epsilon$  space-time dimensions. While the leading poles of loop integrals are scheme-independent, cancellations of these poles with scheme-dependent  $\mathcal{O}(\epsilon)$  terms, resulting from the Dirac algebra in dimensional regularisation, will lead to scheme-dependent finite parts. It should be stressed that, in this context, the finite terms can be of the same order as the logarithmically enhanced ones (as shown in [8]), thus they are phenomenologically relevant. Since four-top operators contribute to  $gg \rightarrow h$  via two-loop diagrams, the finite terms are expected to be scheme-dependent. Moreover, we find a divergence which depends on the scheme, signaling a scheme-dependent anomalous dimension. We describe in detail how such divergence can be traced back to a finite term (that is expected to be scheme-dependent) in one of the one-loop subamplitudes entering the computation. We also review the results in naive dimensional regularisation [18] with respect to the ones obtained in Ref. [8] and we discuss various subtleties that arise in the comparison with the *Breitenlohner-Maison-’t Hooft-Veltman* scheme [19, 20] for the treatment of  $\gamma_5$ .

Furthermore, we point out that building the SMEFT expansion on the counting of the canonical dimension alone can lead to inconsistencies, as has been explained in Ref. [21]. In a counting scheme that in addition takes into account whether an operator is potentially loop-generated, the four-top operators and the chromomagnetic operator enter the Higgs-gluon coupling at the same order [22–29] and therefore should not be considered in isolation.

Our paper is structured as follows: in Sec. II we in-

\* stefano.dinoi@phd.unipd.it

† ramona.groeber@pd.infn.it

‡ gudrun.heinrich@kit.edu

§ jannis.lang@kit.edu

¶ marco.vitti@unipd.it

roduce the operators considered in our analysis and we fix our notation. In Sec. III we discuss different schemes for the  $D$ -dimensional continuation of  $\gamma_5$ . Section IV is devoted to the computation of one-loop subamplitudes required to obtain the result for the  $gg \rightarrow h$  amplitude including the operators given in Sec. II. The two different schemes are then used for the computation of the  $gg \rightarrow h$  rate presented in Sec. V. We also discuss how the scheme-dependence of the parameters of the theory compensates for the scheme-dependence of the matrix elements, providing a scheme-independent physical result. In Sec. VI we validate our approach by means of a matching with two simple models. In Sec. VII we briefly show that a non trivial interplay exists not only in the case of four-top operators, as detailed in this work, but also when other operators containing chiral vertices are involved. In App. A we show the result we obtain for  $\Gamma(h \rightarrow \bar{b}b)$  as a side-product of our analysis, commenting also in this case about the scheme-independence of the result. In App. B we discuss the relation between the counterterms and the anomalous dimension matrix, highlighting some subtleties that arise when dimensional regularisation is used. In App. C we report the scheme-independent part of the  $gg \rightarrow h$  amplitude and in App. D we give the Feynman rules needed for our computation.

## II. SETUP

If the new physics scale  $\Lambda$  is assumed to be much larger than the electroweak scale, new physics can be described in terms of an EFT. In this paper we use the SMEFT, where all SM fields transform under the SM symmetries, including the scalar field  $\phi$  which contains the Higgs boson. At dimension-five level there is only the lepton-number violating ‘‘Weinberg’’ operator responsible for Majorana mass generation of neutrinos [30], so the dominant new physics effects relevant in collider physics are described by dimension-six operators:

$$\mathcal{L}_{\mathcal{D}=6} = \mathcal{L}_{\text{SM}} + \frac{1}{\Lambda^2} \sum_i \mathcal{C}_i \mathcal{O}_i, \quad (1)$$

where  $\mathcal{O}_i$  denotes every possible non-redundant combination of SM fields with mass dimension six that preserves the symmetries of the SM. A complete basis of dimension-six operators was presented for the first time in Ref. [2], the so-called *Warsaw basis*, that we will adopt in the following. In the Warsaw basis redundant operators are eliminated making use of field redefinitions, integration-by-part identities and Fierz identities.

We are mostly interested in the effect of the four-top operators on Higgs production via gluon fusion (as well as the Higgs decay to gluons). The operators that lead

to four-top interactions are given by

$$\begin{aligned} \mathcal{L}_{4t} = & \frac{\mathcal{C}_{QQ}^{(1)}}{\Lambda^2} (\bar{Q}_L \gamma_\mu Q_L) (\bar{Q}_L \gamma^\mu Q_L) \\ & + \frac{\mathcal{C}_{QQ}^{(3)}}{\Lambda^2} (\bar{Q}_L \tau^I \gamma_\mu Q_L) (\bar{Q}_L \tau^I \gamma^\mu Q_L) \\ & + \frac{\mathcal{C}_{Qt}^{(1)}}{\Lambda^2} (\bar{Q}_L \gamma_\mu Q_L) (\bar{t}_R \gamma^\mu t_R) \\ & + \frac{\mathcal{C}_{Qt}^{(8)}}{\Lambda^2} (\bar{Q}_L T^A \gamma_\mu Q_L) (\bar{t}_R T^A \gamma^\mu t_R) \\ & + \frac{\mathcal{C}_{tt}}{\Lambda^2} (\bar{t}_R \gamma_\mu t_R) (\bar{t}_R \gamma^\mu t_R). \end{aligned} \quad (2)$$

The field  $Q_L$  stands here for the  $SU(2)_L$  doublet of the third quark generation,  $t_R$  for the right-handed top quark field. The  $SU(3)_c$  generators are denoted as  $T^A$  while  $\tau^I$  are the Pauli matrices. We assume all the Wilson coefficients to be real, since we are not interested in CP-violating effects.

The operators in Eq. (2) contribute to the  $gg \rightarrow h$  amplitude via two-loop diagrams. At one-loop and tree-level, respectively, the following operators contribute to the (CP-even) Higgs-gluon coupling

$$\begin{aligned} \mathcal{L}_{2t} = & \left[ \frac{\mathcal{C}_{t\phi}}{\Lambda^2} (\bar{Q}_L \tilde{\phi} t_R) \phi^\dagger \phi + \frac{\mathcal{C}_{tG}}{\Lambda^2} \bar{Q}_L \sigma^{\mu\nu} T^A t_R \tilde{\phi} G_{\mu\nu}^A + \text{H.c.} \right], \\ \mathcal{L}_s = & \frac{\mathcal{C}_{\phi G}}{\Lambda^2} \phi^\dagger \phi G_{\mu\nu} G^{\mu\nu}, \end{aligned} \quad (3)$$

where  $G_{\mu\nu}$  is the gluon field strength tensor,  $\tilde{\phi} = i\tau^2 \phi^*$  and  $\sigma_{\mu\nu} = i/2[\gamma_\mu, \gamma_\nu]$ .

To summarise our EFT setup, our Lagrangian reads:

$$\mathcal{L}_{\mathcal{D}=6} = \mathcal{L}_{\text{SM}} + \mathcal{L}_{4t} + \mathcal{L}_{2t} + \mathcal{L}_s. \quad (4)$$

We follow Ref. [31] for what concerns the conventions in  $\mathcal{L}_{\text{SM}}$ ,

$$\begin{aligned} \mathcal{L}_{\text{SM}} = & -\frac{1}{4} G_{\mu\nu}^A G^{A\mu\nu} - \frac{1}{4} W_{\mu\nu}^I W^{I\mu\nu} - \frac{1}{4} B_{\mu\nu} B^{\mu\nu} \\ & + \sum_\psi \bar{\psi} i \not{D} \psi + (D_\mu \phi)^\dagger (D^\mu \phi) \\ & - \lambda \left( \phi^\dagger \phi - \frac{1}{2} v^2 \right)^2 - Y_u \tilde{\phi}^\dagger \bar{u}_R Q_L + \text{H.c.} \end{aligned} \quad (5)$$

When spontaneous symmetry breaking occurs ( $\phi = (1/\sqrt{2})(0, (v+h))^T$  in the unitary gauge) one has:

$$\mathcal{L}_{\mathcal{D}=6} \supset -m_t \bar{t} t - g_{h\bar{t}t} h \bar{t} t, \quad (6)$$

where the top mass and the  $h\bar{t}t$  coupling are modified according to

$$\begin{aligned} m_t = & \frac{v}{\sqrt{2}} \left( Y_t - \frac{v^2 \mathcal{C}_{t\phi}}{2 \Lambda^2} \right), \\ g_{h\bar{t}t} = & \frac{1}{\sqrt{2}} \left( Y_t - \frac{3v^2 \mathcal{C}_{t\phi}}{2 \Lambda^2} \right) = \frac{m_t}{v} - \frac{v^2 \mathcal{C}_{t\phi}}{\sqrt{2} \Lambda^2}. \end{aligned} \quad (7)$$

This establishes a connection between  $m_t, g_{h\bar{t}t}$  (broken phase) and  $Y_t, \mathcal{C}_{t\phi}/\Lambda^2$  (unbroken phase).

### III. CONTINUATION SCHEMES FOR $\gamma_5$ TO $D$ DIMENSIONS

Due to the presence of four-fermion operators with different chiralities,  $\gamma_5$  matrices will be present in our loop computations. As well known, the treatment of  $\gamma_5$  in dimensional regularisation is highly non-trivial, as  $\gamma_5$  is an intrinsically four-dimensional object [32]. In this paper, we will consider two different schemes for the  $\gamma_5$  matrix in dimensional regularisation with  $D = 4 - 2\epsilon$ : naive dimensional regularisation (NDR) [18] and the Breitenlohner-Maison-t'Hooft-Veltman scheme (BMHV) [19, 20].

#### A. Naive Dimensional Regularisation

The NDR scheme assumes that the usual anti-commutation relations valid in four dimensions hold also in  $D$  dimensions

$$\{\gamma_\mu, \gamma_\nu\} = 2g_{\mu\nu}, \quad \{\gamma_\mu, \gamma_5\} = 0, \quad \gamma_5^2 = \mathbb{1}. \quad (8)$$

This is inconsistent with the cyclicity of the trace. Assuming that the usual four-dimensional relation

$$\text{Tr}[\gamma_\mu \gamma_\nu \gamma_\rho \gamma_\sigma \gamma_5] = -4i\epsilon_{\mu\nu\rho\sigma} \quad (9)$$

holds, leads to

$$\text{Tr}[\gamma_{\mu_1} \gamma_{\mu_2} \dots \gamma_{\mu_{2n}} \gamma_5] = \text{Tr}[\gamma_{\mu_2} \dots \gamma_{\mu_{2n}} \gamma_5 \gamma_{\mu_1}] + \mathcal{O}(\epsilon), \quad (10)$$

for  $n \geq 3$ . The cyclicity is hence no longer preserved and the computation of a Feynman diagram depends on the starting point of reading in a fermion trace. As was shown in Refs. [33, 34], the NDR scheme in presence of Dirac traces with an odd number of  $\gamma_5$  matrices and at least six  $\gamma$ -matrices only leads to consistent results if the reading point is fixed univocally for all Feynman diagrams.<sup>1</sup>

#### B. Breitenlohner-Maison-'t Hooft-Veltman Scheme

The BMHV scheme divides the algebra in a four-dimensional part and a  $(D-4)$ -dimensional one by defining

$$\begin{aligned} \gamma_\mu^{(D)} &= \gamma_\mu^{(4)} + \gamma_\mu^{(D-4)}, \\ \{\gamma_\mu^{(4)}, \gamma_5\} &= 0, \quad [\gamma_\mu^{(D-4)}, \gamma_5] = 0. \end{aligned} \quad (11)$$

<sup>1</sup> It was shown recently in Ref. [35] that in a computation of the singlet axial-current operator at  $\mathcal{O}(\alpha_s^3)$  between two gluons and the vacuum a revised version of the scheme of Refs. [33, 34] becomes necessary.

For the vertices involving chiral projectors we use the following rule, valid in the BMHV scheme:

$$\gamma_\mu^{(4)}(1 \mp \gamma_5) \rightarrow \frac{1}{2}(1 \pm \gamma_5)\gamma_\mu^{(D)}(1 \mp \gamma_5), \quad (13)$$

which is the most symmetric choice and preserves chirality of the external fields in  $D$  dimensions (see e.g. Refs. [36–38]).

### IV. SCHEME-DEPENDENT FINITE MIXING AT ONE-LOOP ORDER

In this section we comment on the interplay between the four-top operators and other operators entering Eq. (4). This interplay will be important in the discussion of single Higgs production in the next section.

In particular, we want to highlight two points. The first one is that there is a finite mixing between the four-top and other operators, coming already from one-loop diagrams, as shown below. This fact implies that it would be inconsistent to study the contribution coming from four-top operators in isolation. The second point is that the above mixing, being finite, depends on the  $\gamma_5$  scheme employed. When combining the one-loop subamplitudes in two-loop diagrams, in principle this could lead to divergent terms that are scheme-dependent. However, provided that both schemes are used consistently, the physical result for the complete two-loop amplitude is expected to be scheme-independent.

Direct evaluation of the contribution of the four-top operators to the  $g \rightarrow \bar{t}t$  amplitude gives a contribution proportional to an insertion of the chromomagnetic operator. Pictorially, this can be represented as follows

$$g \text{ (gluon) } \rightarrow \bar{t}t \text{ (fermion loop with red dot)} = \frac{\mathcal{C}_{Qt}^{(1)} - \frac{1}{8}\mathcal{C}_{Qt}^{(8)}}{\mathcal{C}_{tG}} K_{tG} \times g \text{ (gluon) } \rightarrow \bar{t}t \text{ (fermion loop with blue dot)}, \quad (14)$$

where the red and blue square dots denote an insertion of four-top and chromomagnetic operators, respectively. The value of  $K_{tG}$  in Eq. (14) depends on the  $\gamma_5$  scheme. We find

$$K_{tG} = \begin{cases} \frac{\sqrt{2}m_t g_s}{16\pi^2 v} & \text{(NDR)} \\ 0 & \text{(BMHV)}. \end{cases} \quad (15)$$

We note that Eq. (14) holds only when the gluon is on shell. In this case, only one of the two possible contractions of the fermion lines, namely the one in Fig. 1b, gives a non-vanishing contribution. We stress that the difference between the two schemes in Eq. (15) does not arise from a trace in Dirac space and therefore cannot be related to trace ambiguities [33].

When we consider other one-loop amplitudes with four-top operator insertions, which will enter as subamplitudes in the  $gg \rightarrow h$  computation, we find again that

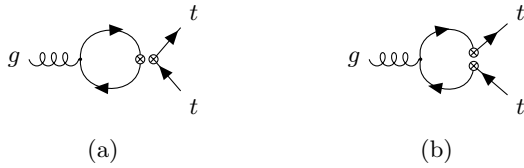


Figure 1: The two possible contractions within four-fermion operators where all the fermions are equal: (a) closed fermion line yielding a trace; (b) open fermion line without any traces.

the finite contributions are scheme-dependent, whereas the divergent parts are equal in the two schemes. In particular, the diagrammatic relation concerning the four-top contribution to the Higgs-top coupling is

$$\begin{aligned}
 & \left. \begin{array}{c} h \text{ --- } \bullet \\ \text{---} \bullet \\ \text{---} \bullet \\ \text{---} \bullet \end{array} \right|_{\text{FIN}} = \frac{1}{\Lambda^2} \left( \mathcal{C}_{Qt}^{(1)} + \frac{4}{3} \mathcal{C}_{Qt}^{(8)} \right) \\
 & \times (B_{h\bar{t}t} + K_{h\bar{t}t}) \times \begin{array}{c} t \\ \text{---} \bullet \\ \text{---} \bullet \\ \text{---} \bullet \end{array}, \quad (16)
 \end{aligned}$$

where we find

$$K_{h\bar{t}t} = \begin{cases} \frac{(m_h^2 - 6m_t^2)}{16\pi^2} & (\text{NDR}) \\ 0 & (\text{BMHV}), \end{cases} \quad (17)$$

and where  $B_{h\bar{t}t}$  is scheme-independent and can be expressed as

$$\begin{aligned}
 B_{h\bar{t}t} = & \frac{m_t^2}{4\pi^2\tau} \times \left( -2\beta^3 \log\left(\frac{\beta-1}{\beta+1}\right) \right. \\
 & \left. + (3\tau-2) \log\left(\frac{\tilde{\mu}^2}{m_t^2}\right) + 5\tau - 4 \right), \quad (18)
 \end{aligned}$$

with

$$\beta = \sqrt{1-\tau}, \quad \tau = \frac{4m_t^2}{m_h^2} \quad (19)$$

and with  $\tilde{\mu}^2 = 4\pi\mu^2 e^{-\gamma_E}$ . We note that  $B_{h\bar{t}t}$  and the analogous  $B$  terms in this paper are scheme-independent once a convention to identify  $K_{h\bar{t}t}$  is defined. For example, in this section we choose the  $B$  terms such that the  $K$ -terms vanish in BMHV. However, this definition is totally arbitrary and does not affect the final results. What is relevant for our purpose is the difference between  $K$ -terms in different schemes, which is insensitive to the convention chosen.

Regarding the corrections to the top quark propagator we find that only the mass term gets corrected. Diagrammatically, we have

$$\begin{aligned}
 & \left. \begin{array}{c} t \text{ --- } \bullet \\ \text{---} \bullet \\ \text{---} \bullet \end{array} \right|_{\text{FIN}} = \frac{1}{\Lambda^2} \left( \mathcal{C}_{Qt}^{(1)} + \frac{4}{3} \mathcal{C}_{Qt}^{(8)} \right) \\
 & \times (B_{m_t} + K_{m_t}) \times \begin{array}{c} t \\ \text{---} \bullet \\ \text{---} \bullet \end{array}, \quad (20)
 \end{aligned}$$

$$K_{m_t} = \begin{cases} -\frac{m_t^2}{8\pi^2} & (\text{NDR}) \\ 0 & (\text{BMHV}). \end{cases} \quad (21)$$

Also in this case,  $B_{m_t}$  is scheme-independent

$$B_{m_t} = m_t^2 \times \frac{\log\left(\frac{\tilde{\mu}^2}{m_t^2}\right) + 1}{4\pi^2}. \quad (22)$$

The results in Eqs. (14, 16, 20) deserve some discussions. Equation (14) shows that the chromomagnetic and four-top operators are closely linked and contribute at the same order in the EFT expansion, even though the latter operators come with an explicit loop diagram. This can be understood from the fact that, under the assumption that the UV-complete theory is renormalisable and that the SM fields are weakly coupled to the unknown fields, there are operators which cannot be generated at tree-level. This means that their Wilson coefficients are expected to contain a loop suppression factor  $1/(4\pi)^2$  [21, 22]. The power counting can be formalised conveniently via the chiral dimension  $d_\chi$ , supplementing the canonical dimension counting in  $1/\Lambda$ . As a result, the tree-level diagram associated with the (loop-generated) operator  $\mathcal{O}_{\phi G}$  enters the  $gg \rightarrow h$  amplitude at the same power as the (tree-generated) operator  $\mathcal{O}_{t\phi}$  inserted into a SM-like loop diagram, which is  $1/(4\pi)^2 1/\Lambda^2$ . Similarly,  $\mathcal{O}_{tG}$  inserted into a one-loop diagram for  $gg \rightarrow h$  (see Fig. 3) and the two-loop diagram stemming from the insertion of the four-top operators into the  $gg \rightarrow h$  matrix element (Fig. 2c) are of the same power, which is  $1/(4\pi)^4 1/\Lambda^2$ . In the former case a loop-generated operator is inserted into a one-loop diagram, while in the latter case a tree-generated operator is contained in an explicit two-loop diagram. Therefore, in Eq. (3),  $\mathcal{C}_{tG}$  contains a loop suppression factor  $1/(4\pi)^2$  relative to  $\mathcal{C}_{t\phi}$ , the same holds for  $\mathcal{C}_{\phi G}$ . Equation (16) shows that  $g_{h\bar{t}t}$  and the four-top operators are also linked, however this relation comes with a relative suppression factor  $1/\Lambda^2 \times 1/(4\pi)^2$ .

## V. CALCULATION OF THE HIGGS-GLUON COUPLING

In this section, we compute the four-top operator contribution at two-loop order to the Higgs-gluon coupling in the two different  $\gamma_5$  schemes introduced in Sec. III. In the previous section we have shown that this contribution cannot be separated from that of the operators of

$\mathcal{L}_{2t}$  in Eq. (3). In the case of  $gg \rightarrow h$ , we express the renormalised amplitude as follows

$$\mathcal{M}_{\text{EFT}} = \frac{1}{\Lambda^2} \{ \mathcal{C}_{4t} \mathcal{M}_{4t} + \mathcal{C}_{tG} \mathcal{M}_{tG} + \mathcal{C}_{\phi G} \mathcal{M}_{\phi G} + \mathcal{C}_{t\phi} \mathcal{M}_{t\phi} + \mathcal{M}_{\text{C.T.}} \}, \quad (23)$$

where the inclusion of  $\mathcal{O}_{\phi G}$  is required in order to cancel the divergent part coming from  $\mathcal{M}_{tG}$ . The total matrix element is given by

$$\mathcal{M}_{\text{TOT}} = \mathcal{M}_{\text{SM}} + \mathcal{M}_{\text{EFT}}. \quad (24)$$

The contribution from  $\mathcal{O}_{t\phi}$  manifests itself as a modification of  $g_{h\bar{t}t}$  and  $m_t$  (see Eq. (7)) entering  $\mathcal{M}_{\text{SM}}$ , so its effect is understood to be included in  $\mathcal{M}_{\text{SM}}$ .

The four-top contribution to  $\mathcal{M}_{\text{EFT}}$  can be split according to the different topologies of the associated Feynman diagrams. In Fig. 2 we show a sample of the 12 diagrams that need to be computed. The first topology is related to a correction to the Higgs-top-quark coupling (2a), the second one to a correction to the top quark propagator (2b) and the third one to a correction to the gluon-top vertex (2c). We generated the diagrams with `qgraf-3.6.5` [39] and performed the algebra with `FeynCalc` [40–42]. Following the above classification, we express the four-top contribution as

$$\begin{aligned} \mathcal{C}_{4t} \mathcal{M}_{4t} &= \mathcal{A}_{g_{h\bar{t}t}+m_t} \left( \mathcal{C}_{Qt}^{(1)} + \frac{4}{3} \mathcal{C}_{Qt}^{(8)} \right) \frac{1}{\Lambda^2} \\ &+ \mathcal{A}_{g_{\bar{t}t}} \left( \mathcal{C}_{Qt}^{(1)} - \frac{1}{6} \mathcal{C}_{Qt}^{(8)} \right) \frac{1}{\Lambda^2}. \end{aligned} \quad (25)$$

The two different combinations of the Wilson coefficients in Eq. (25) arise from the colour algebra. We find that the result of  $\mathcal{A}_{g_{\bar{t}t}}$  can be expressed in terms of the contribution to the amplitude due to an insertion of the chromomagnetic operator

$$\mathcal{A}_{g_{\bar{t}t}} = \left[ \frac{1}{2} K_{tG} \mathcal{M}_{tG}|_{\text{DIV}} + K_{tG} \mathcal{M}_{tG}|_{\text{FIN}} \right], \quad (26)$$

where  $K_{tG}$  is the same as in Eq. (15). The divergent and finite parts of  $\mathcal{M}_{tG}$  are given, respectively, by ( $A_1, A_2$  being the colour indices of the gluons)

$$\mathcal{M}_{tG}|_{\text{DIV}} = -g_s m_t \frac{1}{\epsilon} \frac{\sqrt{2}}{2\pi^2} L^{\mu_1 \mu_2} \epsilon_{\mu_1}(p_1) \epsilon_{\mu_2}(p_2) \delta^{A_1 A_2}, \quad (27)$$

$$\begin{aligned} \mathcal{M}_{tG}|_{\text{FIN}} &= -\frac{g_s m_t \sqrt{2}}{4\pi^2} L^{\mu_1 \mu_2} \epsilon_{\mu_1}(p_1) \epsilon_{\mu_2}(p_2) \delta^{A_1 A_2} \\ &\times \left( \frac{1}{4} \tau \log^2 \left( \frac{\beta-1}{\beta+1} \right) + \beta \log \left( \frac{\beta-1}{\beta+1} \right) \right. \\ &\left. + 2 \log \left( \frac{\tilde{\mu}^2}{m_t^2} \right) + 1 \right), \end{aligned} \quad (28)$$

with

$$L^{\mu_1 \mu_2} = (m_h^2/2 g^{\mu_1 \mu_2} - p_1^{\mu_2} p_2^{\mu_1}). \quad (29)$$

We point out that the fact that  $K_{tG}$  factorises in Eq. (26) does not depend on the scheme. The value of  $K_{tG}$  depends on the scheme, and in particular  $K_{tG} = 0$  in BMHV. Remarkably, this implies that the structure of the divergences is different between the two schemes. This happens because of the combination of a scheme-independent pole of a loop integral with the scheme-dependent finite terms in Eq. (14). On the other hand, we find that the divergent terms in  $\mathcal{A}_{g_{h\bar{t}t}+m_t}$  are scheme-independent.

## A. Renormalisation

We use the minimal subtraction (MS) renormalisation prescription for all the parameters in the theory. Schematically, the counterterms needed to renormalise the amplitude are given by

$$\mathcal{M}_{\text{C.T.}} = \begin{array}{c} g \text{---} \text{---} h \\ \text{---} \text{---} \\ g \text{---} \text{---} \end{array} + \begin{array}{c} g \text{---} \text{---} h \\ \text{---} \text{---} \\ g \text{---} \text{---} \end{array} + \begin{array}{c} g \text{---} \text{---} h \\ \text{---} \text{---} \\ g \text{---} \text{---} \end{array}. \quad (30)$$

For the top quark mass we have

$$m_t^{\text{MS}} = m_t^{(0)} + \delta m_t, \quad (31)$$

with

$$\delta m_t = \frac{m_t^3}{4\pi^2 \Lambda^2 \epsilon} \left( \mathcal{C}_{Qt}^{(1)} + \frac{4}{3} \mathcal{C}_{Qt}^{(8)} \right). \quad (32)$$

We note that typically in the computation of  $gg \rightarrow h$  the top quark mass is renormalised in the on-shell scheme. In order to simplify our point (as we find the same MS counterterm in NDR and BMHV) we restrict the discussion here to a pure MS renormalisation.

In addition, the Wilson coefficient  $\mathcal{C}_{t\phi}$ , which mixes with the four-top operators via renormalisation group equation (RGE) running, needs to be renormalised. The coefficient of the operator is renormalised according to

$$\mathcal{C}_{t\phi}^{\text{MS}} = \mathcal{C}_{t\phi}^{(0)} + \delta \mathcal{C}_{t\phi} \quad \text{with} \quad \delta \mathcal{C}_{t\phi} = -\frac{1}{2\epsilon} \frac{1}{16\pi^2} \gamma_{t\phi,j} \mathcal{C}_j, \quad (33)$$

where  $\gamma$  denotes the one-loop anomalous dimension of the SMEFT. The entries relevant for our discussion can be obtained from Refs. [43, 44]. The equation correlating  $\delta \mathcal{C}_{t\phi}$  and the anomalous dimension matrix in Eq. (33) is discussed in detail in App. B. The only four-top Wilson coefficients contributing to  $\gamma_{t\phi,j} \mathcal{C}_j$  are  $\mathcal{C}_{Qt}^{(1,8)}$ . The operator  $\mathcal{O}_{t\phi}$  modifies the Higgs couplings to top quarks as discussed previously, see Eq. (7).

In analogy to  $m_t$ , we have:

$$g_{h\bar{t}t}^{\text{MS}} = g_{h\bar{t}t}^{(0)} + \delta g_{h\bar{t}t}, \quad (34)$$

with

$$\delta g_{h\bar{t}t} = g_{h\bar{t}t} \frac{(6m_t^2 - m_h^2)}{8\pi^2 \Lambda^2 \epsilon} \left( \mathcal{C}_{Qt}^{(1)} + \frac{4}{3} \mathcal{C}_{Qt}^{(8)} \right). \quad (35)$$

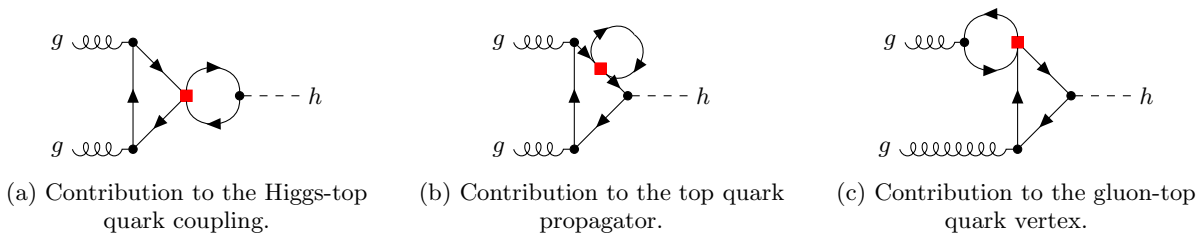


Figure 2: Contributions from insertions of four-top quark operators (red square dot) to  $gg \rightarrow h$  at two-loop level.

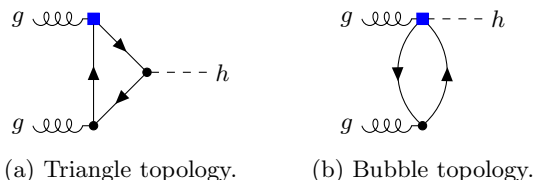


Figure 3: Contribution to the Higgs-top quark coupling with a single insertion of the chromomagnetic operator (blue square dot).

From now on we will drop the superscript MS, leaving understood that all the parameters are renormalised in the MS scheme. We recall that the divergent parts of the diagrams in Figs. 2a and 2b are equal in the NDR and BMHV schemes, and they are fully removed by one-loop diagrams with an insertion of the one-loop counterterms in Eqs. (32), (35).

The insertion of the chromomagnetic operator (see Fig. 3) gives a divergent contribution to the Higgs-gluon coupling at one loop [44–46]. We find this contribution to be scheme-independent. To remove all the divergences we need to choose (see Eq. (26))

$$\delta_{\phi G} = \frac{g_{h\bar{t}t}g_s}{\Lambda^2\epsilon 4\sqrt{2}\pi^2} \left( \mathcal{C}_{tG} + \frac{K_{tG}}{2} \left( \mathcal{C}_{Qt}^{(1)} - \frac{1}{6}\mathcal{C}_{Qt}^{(8)} \right) \right). \quad (36)$$

This entails an important consequence: the anomalous dimension is scheme-dependent, as it contains the scheme-dependent  $K_{tG}$ . From  $d\mathcal{C}_{\phi G}^{(0)}/d\mu = 0$ , we obtain

$$16\pi^2\mu \frac{d\mathcal{C}_{\phi G}}{d\mu} = -4\sqrt{2}g_{h\bar{t}t}g_s \left( \mathcal{C}_{tG} + K_{tG} \left( \mathcal{C}_{Qt}^{(1)} - \frac{1}{6}\mathcal{C}_{Qt}^{(8)} \right) \right). \quad (37)$$

Notice that there is a relative factor of 2 between the contributions from  $\mathcal{C}_{Qt}^{(1,8)}$  in Eq. (36) and Eq. (37). This is a consequence of the contribution proportional to  $\mathcal{C}_{tG}$  being  $\mathcal{O}(g_{h\bar{t}t}g_s)$  and the contribution proportional to  $\mathcal{C}_{Qt}^{(1,8)}$  being  $\mathcal{O}(g_{h\bar{t}t}^2g_s^2)$ .<sup>2</sup> This (merely algebraic) fact will have important consequences, as we will show in the following. The details can be found in App. B. We stress that the

form of the RGE in Eq. (37) shows that the contributions of  $\mathcal{C}_{tG}$ ,  $\mathcal{C}_{Qt}^{(1,8)}$  enter at different loop orders (being  $K_{tG} = \mathcal{O}(1/(4\pi)^2)$ ). However, when the loop counting from Ref. [21] is considered, they enter at the same order, as explained in Sec. IV.

The differences in NDR and BMHV originating from the finite mixing of the four-fermion operators with chiral structure  $(\bar{L}L)(\bar{R}R)$  into the chromomagnetic operator are well known, in particular in the context of flavour physics. This effect can induce a scheme-dependent anomalous dimension matrix at leading order [47–51]. Using the strategy proposed in [36, 47, 49], we can perform a finite renormalisation of the chromomagnetic operator and write

$$\mathcal{C}_{tG} \rightarrow \mathcal{C}_{tG} + K_{tG} \left( \mathcal{C}_{Qt}^{(1)} - \frac{1}{6}\mathcal{C}_{Qt}^{(8)} \right). \quad (38)$$

This choice ensures a scheme-independent anomalous dimension matrix.

## B. Renormalised amplitude

In the previous section we discussed how to obtain the same anomalous dimension matrix in both schemes. This is achieved via the inclusion of the effects of a scheme-dependent finite mixing in the Wilson coefficients. These effects are related to one-loop subdiagrams as in Eq. (14). One may wonder if redefinitions similar to Eq. (38) are enough to obtain the same result for the finite part of the amplitude in both schemes. In other words, we want to check if the scheme-dependence of the two-loop amplitude can be accounted for simply by computing one-loop subdiagrams. The only scheme-dependent terms in the amplitudes are the ones stemming from a two-loop insertion of the four-top operators and they are parametrised by  $K_{tG}$ ,  $K_{g_{h\bar{t}t}}$  and  $K_{m_t}$ .

We express the renormalised contribution from the diagrams in Figs. 2a, 2b as

$$\mathcal{A}_{g_{h\bar{t}t}+m_t}^{\text{Ren}} = \mathcal{M}_{g_{h\bar{t}t}+m_t}^{\text{S.I.}} + K_{g_{h\bar{t}t}}\mathcal{M}^{\text{SM}} + K_{m_t}\frac{\partial\mathcal{M}^{\text{SM}}}{\partial m_t} \times m_t, \quad (39)$$

where  $\mathcal{M}^{\text{SM}}$ ,  $\mathcal{M}_{g_{h\bar{t}t}+m_t}^{\text{S.I.}}$  are scheme-independent and they can be found in App. C. Putting together

<sup>2</sup> Using  $g_{h\bar{t}t} = m_t/v + \mathcal{O}(1/\Lambda^2)$ .

Eqs. (25),(26) and (39) we have the following expression for the renormalised matrix element

$$\begin{aligned}
\mathcal{M}_{\text{TOT}}^{\text{Ren}} &= \left( \mathcal{C}_{Qt}^{(1)} + \frac{4}{3} \mathcal{C}_{Qt}^{(8)} \right) \frac{1}{\Lambda^2} \mathcal{M}_{g_{h\bar{t}t}+m_t}^{\text{S.I.}} \\
&+ \left[ \mathcal{C}_{tG} + \left( \mathcal{C}_{Qt}^{(1)} - \frac{1}{6} \mathcal{C}_{Qt}^{(8)} \right) K_{tG} \right] \frac{1}{\Lambda^2} \mathcal{M}_{tG}|_{\text{FIN}} \\
&+ \left[ 1 + \left( \mathcal{C}_{Qt}^{(1)} + \frac{4}{3} \mathcal{C}_{Qt}^{(8)} \right) \frac{1}{\Lambda^2} K_{h\bar{t}t} \right] \mathcal{M}_{\text{SM}} \\
&+ \left( \mathcal{C}_{Qt}^{(1)} + \frac{4}{3} \mathcal{C}_{Qt}^{(8)} \right) \frac{1}{\Lambda^2} K_{m_t} \frac{\partial \mathcal{M}_{\text{SM}}}{\partial m_t} \times m_t \\
&+ \mathcal{C}_{\phi G} \mathcal{M}_{\phi G} \frac{1}{\Lambda^2}.
\end{aligned} \tag{40}$$

We note that  $\mathcal{M}_{\text{TOT}}^{\text{Ren}}$  represents a physical on-shell scattering amplitude, which must be scheme-independent.<sup>3</sup> Therefore, the scheme-dependence of the  $K$ -terms has to be compensated by a scheme-dependence of the parameters. To make this more evident, we define the following set of parameters identified by a tilde

$$\tilde{\mathcal{C}}_{tG} = \mathcal{C}_{tG} + \left( \mathcal{C}_{Qt}^{(1)} - \frac{1}{6} \mathcal{C}_{Qt}^{(8)} \right) K_{tG}, \tag{41}$$

$$\tilde{g}_{h\bar{t}t} = g_{h\bar{t}t} \left[ 1 + \left( \mathcal{C}_{Qt}^{(1)} + \frac{4}{3} \mathcal{C}_{Qt}^{(8)} \right) \frac{1}{\Lambda^2} K_{h\bar{t}t} \right], \tag{42}$$

$$\tilde{m}_t = m_t \left[ 1 + \left( \mathcal{C}_{Qt}^{(1)} + \frac{4}{3} \mathcal{C}_{Qt}^{(8)} \right) \frac{1}{\Lambda^2} K_m \right]. \tag{43}$$

Noting that, under a redefinition of the top mass  $m_t \rightarrow m_t + \Delta m_t$ , one has  $\mathcal{M}_{\text{SM}} \rightarrow \mathcal{M}_{\text{SM}} + \Delta m_t \partial \mathcal{M}_{\text{SM}} / \partial m_t$ , we can write the total matrix element in a more compact form (at  $\mathcal{O}(1/\Lambda^2)$ ):

$$\begin{aligned}
\mathcal{M}_{\text{TOT}}^{\text{Ren}} &= \left( \mathcal{C}_{Qt}^{(1)} + \frac{4}{3} \mathcal{C}_{Qt}^{(8)} \right) \frac{1}{\Lambda^2} \mathcal{M}_{g_{h\bar{t}t}+m_t}^{\text{S.I.}} \\
&+ \frac{\tilde{\mathcal{C}}_{tG}}{\Lambda^2} \mathcal{M}_{tG}|_{\text{FIN}} + \mathcal{M}_{\text{SM}}(\tilde{g}_{h\bar{t}t}, \tilde{m}_t) + \frac{\mathcal{C}_{\phi G}}{\Lambda^2} \mathcal{M}_{\phi G}.
\end{aligned} \tag{44}$$

In the previous expression,  $\mathcal{M}_{\text{SM}}(\tilde{g}_{h\bar{t}t}, \tilde{m}_t)$  is given by Eq. (C2) where  $g_{h\bar{t}t}$ ,  $m_t$  are replaced by  $\tilde{g}_{h\bar{t}t}$ ,  $\tilde{m}_t$ . From the amplitudes  $\mathcal{M}_{g_{h\bar{t}t}+m_t}^{\text{S.I.}}$ ,  $\mathcal{M}_{tG}$ ,  $\mathcal{M}_{\text{SM}}$ ,  $\mathcal{M}_{\phi G}$  being scheme-independent, it follows that the combinations in Eqs. (41-43) must be scheme-independent.

It should be stressed that Eq. (41) is the same relation we obtained in the previous section, namely Eq. (38): the same finite shift makes both the anomalous dimension matrix and the renormalised amplitude scheme-independent. We also remark that, at the order we are working,  $g_{h\bar{t}t}$  and  $m_t$  can be used interchangeably with  $\tilde{g}_{h\bar{t}t}$  and  $\tilde{m}_t$  in  $\mathcal{M}_{tG, \phi G}$ ,  $\mathcal{M}_{g_{h\bar{t}t}+m_t}^{\text{S.I.}}$  because their contribution to  $\mathcal{M}_{\text{TOT}}$  is already suppressed by  $\mathcal{O}(1/\Lambda^2)$ .

<sup>3</sup> This can be best understood from a top-down perspective.

## C. Summary of the computation

We can now summarize the differences between the two schemes. From Eqs. (41-43) it is evident that there exists a difference between the parameters in the two schemes which is proportional to  $K_X^{\text{NDR}} - K_X^{\text{BMHV}}$ . This quantity does not depend on the prescription used to identify the  $K$ -terms.

In BMHV all the  $K$ -terms are vanishing, so the previous redefinitions are trivial. The scheme-independence condition  $\tilde{X}_i^{\text{NDR}} = \tilde{X}_i^{\text{BMHV}}$  allows us to write at  $\mathcal{O}(1/\Lambda^2)$ <sup>4</sup>

$$\mathcal{C}_{tG}^{\text{NDR}} = \mathcal{C}_{tG}^{\text{BMHV}} - \left( \mathcal{C}_{Qt}^{(1)} - \frac{1}{6} \mathcal{C}_{Qt}^{(8)} \right) \frac{\sqrt{2} g_{h\bar{t}t} g_s}{16\pi^2}, \tag{45}$$

$$g_{h\bar{t}t}^{\text{NDR}} = g_{h\bar{t}t}^{\text{BMHV}} - g_{h\bar{t}t} \left( \mathcal{C}_{Qt}^{(1)} + \frac{4}{3} \mathcal{C}_{Qt}^{(8)} \right) \frac{(m_h^2 - 6m_t^2)}{16\pi^2 \Lambda^2}, \tag{46}$$

$$m_t^{\text{NDR}} = m_t^{\text{BMHV}} + \left( \mathcal{C}_{Qt}^{(1)} + \frac{4}{3} \mathcal{C}_{Qt}^{(8)} \right) \frac{m_t^3}{8\pi^2 \Lambda^2}. \tag{47}$$

The map described by Eqs. (45-47), establishes a connection between the two schemes. When such relations are considered, the two schemes give the same anomalous dimension matrix and the same renormalised amplitude.

## VI. MATCHING WITH UV-MODELS

As discussed in the previous section, the differences in the finite terms of the amplitude when using the NDR and the BMHV scheme can be absorbed by different definitions of the parameters  $\mathcal{C}_{tG}$ ,  $g_{h\bar{t}t}$ , and  $m_t$ . In this section we perform the matching with concrete UV completions of the SM, in order to validate our EFT approach from a top-down point of view. The matching is performed in the unbroken phase (following the notation used in Ref. [52]), in which  $g_{h\bar{t}t}$  and  $m_t$  can be traded more conveniently in favour of  $\mathcal{C}_{t\phi}$  and  $Y_t$ . In the remainder of the section we will use a thicker fermion line to denote the iso-doublet  $Q_L$  and a thinner fermion line to denote the iso-singlet  $t_R$  in the Feynman diagrams.

### A. New scalar: $\Phi \sim (8, 2)_{\frac{1}{2}}$

We consider, in addition to the SM, a new heavy scalar with a mass  $M_\Phi \gg v$  and quantum numbers  $\Phi \sim (8, 2)_{\frac{1}{2}}$ .

<sup>4</sup> If we had included the loop factor  $1/(4\pi)^2$  explicitly in the  $\mathcal{C}_{tG}$ -term in the Lagrangian Eq. (3), it would be manifest that the chromomagnetic and the four-top operators contribute at the same order in the chiral counting, because in this case the factor  $1/(4\pi)^2$  in (45) would be absent.

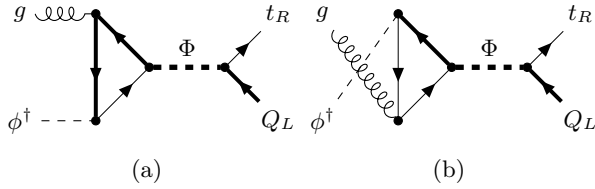


Figure 4: One-loop diagrams contributing to the matching with the chromomagnetic operator.

The Lagrangian in this case can be written as

$$\begin{aligned} \mathcal{L}_\Phi &= (D_\mu \Phi)^\dagger D^\mu \Phi - M_\Phi^2 \Phi^\dagger \Phi \\ &\quad - Y_\Phi (\Phi^{A,\dagger} \varepsilon \bar{Q}_L^T T^A t_R + \text{H.c.}), \end{aligned} \quad (48)$$

where  $\varepsilon$  is the Levi-Civita pseudotensor in the isospin space and  $T$  refers to the transposition in isospin space only. The tree-level matching yields

$$\mathcal{L} = \frac{Y_\Phi^2}{M_\Phi^2} (\bar{Q}_L T^A t_R) (\bar{t}_R T^A Q_L). \quad (49)$$

This operator does not appear in the Warsaw basis since it is considered redundant in  $D = 4$  dimensions. In the following it will be referred to as  $\mathcal{R}_{Q_t}^{(8)}$ . Using the Fierz identities, one can recast this result in terms of operators in the Warsaw basis [52]:

$$\frac{\mathcal{C}_{Q_t}^{(1)}}{\Lambda^2} = -\frac{2}{9} \frac{Y_\Phi^2}{M_\Phi^2}, \quad \frac{\mathcal{C}_{Q_t}^{(8)}}{\Lambda^2} = \frac{1}{6} \frac{Y_\Phi^2}{M_\Phi^2}. \quad (50)$$

Now we compute the matching at one-loop level to the chromomagnetic operator. The relevant diagrams are given in Fig. 4, while diagrams with  $t$ -channel exchange within the loop are forbidden due to the conservation of hypercharge.

Evaluating the diagrams in Fig. 4 gives zero in both NDR and BMHV, in contrast with our previous observations. However, the Fierz identity we used for the matching of the four-fermion operators is broken by  $\mathcal{O}(\epsilon)$  terms when dimensional regularisation is used ( $D = 4 - 2\epsilon$ ), as noted in Ref. [53]. Following this reference, we define the evanescent operator as

$$\mathcal{E} = \mathcal{R}_{Q_t}^{(8)} - \left( -\frac{2}{9} \mathcal{O}_{Q_t}^{(1)} + \frac{1}{6} \mathcal{O}_{Q_t}^{(8)} \right) \quad (51)$$

and we compute its insertion (in both schemes). We find that in NDR the evanescent operator contributes to the matching to the chromomagnetic operator:

$$\begin{aligned} \mathcal{C}_{Q_t}^{(8),R} \mathcal{R}_{Q_t}^{(8)} &= -\frac{2}{9} \frac{Y_\Phi^2}{M_\Phi^2} \mathcal{O}_{Q_t}^{(1)} + \frac{1}{6} \frac{Y_\Phi^2}{M_\Phi^2} \mathcal{O}_{Q_t}^{(8)} \\ &\quad + \underbrace{\frac{1}{16\pi^2} \frac{Y_\Phi^2}{M_\Phi^2} \frac{g_s Y_t}{4}}_{\mathcal{C}_{tG}/\Lambda^2} \mathcal{O}_{tG} + \text{H.c.} \end{aligned} \quad (52)$$

This result reproduces the term proportional to the chromomagnetic operator presented in [53].<sup>5</sup> In BMHV we obtain

$$\mathcal{C}_{Q_t}^{(8),R} \mathcal{R}_{Q_t}^{(8)} = -\frac{\mathcal{C}_{Q_t}^{(1)}/\Lambda^2}{9} \frac{Y_\Phi^2}{M_\Phi^2} \mathcal{O}_{Q_t}^{(1)} + \frac{\mathcal{C}_{Q_t}^{(8)}/\Lambda^2}{6} \frac{Y_\Phi^2}{M_\Phi^2} \mathcal{O}_{Q_t}^{(8)}. \quad (53)$$

We conclude that the difference between the NDR scheme and BMHV scheme (using Eq. (50) and  $\sqrt{2} m_t = Y_t v + \mathcal{O}(1/\Lambda^2)$ ) is exactly the one described by Eq. (45).

Furthermore, we need to compute the matching to the top Yukawa coupling as well as to  $\mathcal{C}_{t\phi}$ . Doing so we find in both schemes zero, by colour. This is in trivial agreement with Eqs. (46), (47) since, within this model,  $\mathcal{C}_{Q_t}^{(1)} + \frac{4}{3} \mathcal{C}_{Q_t}^{(8)} = 0$ . In order to test Eqs. (46), (47) we hence need to consider a different model, namely replacing the colour octet  $\Phi$  with a colour singlet  $\varphi$ .

### B. New scalar: $\varphi \sim (1, 2)_{\frac{1}{2}}$

We consider, in addition to the SM, a new heavy scalar with a mass  $M_\varphi \gg v$  and quantum numbers  $\varphi \sim (1, 2)_{\frac{1}{2}}$ . The Lagrangian in this case can be written as

$$\begin{aligned} \mathcal{L}_\varphi &= (D_\mu \varphi)^\dagger D^\mu \varphi - M_\varphi^2 \varphi^\dagger \varphi \\ &\quad - Y_\varphi (\varphi^\dagger \varepsilon \bar{Q}_L^T t_R + \text{H.c.}). \end{aligned} \quad (54)$$

The tree-level matching yields

$$\mathcal{L} = \frac{Y_\varphi^2}{M_\varphi^2} (\bar{Q}_L t_R) (\bar{t}_R Q_L). \quad (55)$$

As in the previous case, this operator does not appear in the Warsaw basis being redundant in  $D = 4$  dimensions. In the following it will be referred to as  $\mathcal{R}_{Q_t}^{(1)}$ . We find

$$\frac{\mathcal{C}_{Q_t}^{(1)}}{\Lambda^2} = -\frac{1}{6} \frac{Y_\varphi^2}{M_\varphi^2}, \quad \frac{\mathcal{C}_{Q_t}^{(8)}}{\Lambda^2} = -\frac{Y_\varphi^2}{M_\varphi^2}. \quad (56)$$

Due to colour structure, there are no contributions to the chromomagnetic operator. The tree-level matching implies  $\mathcal{C}_{Q_t}^{(1)} - \frac{1}{6} \mathcal{C}_{Q_t}^{(8)} = 0$ , in agreement with Eq. (45) since  $\mathcal{C}_{tG}^{\text{NDR}} = \mathcal{C}_{tG}^{\text{BMHV}} = 0$  within this model.

Following the procedure outlined in the previous section, we compute the diagrams in Fig. 5 to compute the

<sup>5</sup> This reference uses a different convention for the covariant derivative with respect to the one used in Ref. [54], which we follow in the Feynman rules. This leads to a relative minus sign in terms with an odd power of  $g_s$ . In addition, the different normalisation of the quartic Higgs self-coupling in Ref. [53] requires the replacements  $\lambda/2 \rightarrow \lambda$ ,  $\mu^2 \rightarrow \lambda v^2$  to convert their result into our conventions.

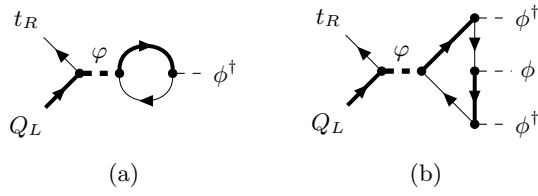


Figure 5: One-loop diagrams contributing to the matching to the Yukawa coupling (left) and to  $\mathcal{C}_{t\phi}$  (right).

contributions to  $Y_t$  and  $\mathcal{C}_{t\phi}$  in both schemes. The matching condition for  $Y_t$  ( $\mathcal{C}_{t\phi}$ ) is obtained subtracting from the diagram in Fig. 5a (5b) the one-loop amplitude for  $\bar{Q}_L t_R \rightarrow \phi^\dagger$  ( $\bar{Q}_L t_R \rightarrow \phi^\dagger \phi \phi^\dagger$ ) with an insertion of four-top operators. In other words, we are interested in computing the insertion of the evanescent operator:

$$\mathcal{E} = \mathcal{R}_{Q_t}^{(1)} - \left( -\frac{1}{6} \mathcal{O}_{Q_t}^{(1)} - \mathcal{O}_{Q_t}^{(8)} \right). \quad (57)$$

In NDR we find:

$$\begin{aligned} \mathcal{C}_{Q_t}^{(1),R} \mathcal{R}_{Q_t}^{(1)} &= -\frac{1}{6} \frac{Y_\phi^2}{M_\phi^2} \mathcal{O}_{Q_t}^{(1)} - \frac{Y_\phi^2}{M_\phi^2} \mathcal{O}_{Q_t}^{(8)} \\ &+ \underbrace{\frac{1}{16\pi^2} \frac{Y_\phi^2}{M_\phi^2} (3Y_t^3 - 3\lambda)}_{\mathcal{C}_{t\phi}/\Lambda^2} \mathcal{O}_{t\phi} + \text{H.c.} \\ &- \underbrace{\frac{1}{16\pi^2} \frac{Y_\phi^2}{M_\phi^2} \frac{3}{2} \lambda v^2}_{\Delta Y_t} (\bar{Q}_L \tilde{\phi} t_R) + \text{H.c.}, \end{aligned} \quad (58)$$

confirming once again the results obtained in [53]. In this notation,  $\Delta Y_t$  represents the contribution to the top Yukawa coupling from the matching, while  $Y_t$  represents the coefficient of the four-dimensional Yukawa operator ( $\bar{Q}_L \tilde{\phi} t_R$ ).

In BMHV we find:

$$\mathcal{C}_{Q_t}^{(1),R} \mathcal{R}_{Q_t}^{(1)} = -\frac{1}{6} \frac{Y_\phi^2}{M_\phi^2} \mathcal{O}_{Q_t}^{(1)} - \frac{Y_\phi^2}{M_\phi^2} \mathcal{O}_{Q_t}^{(8)}. \quad (59)$$

Using the well known relations Eq. (7) we can compute  $m_t$ ,  $g_{ht\bar{t}}$  and confirm Eqs. (46), (47).

## VII. INTERPLAY BETWEEN MORE OPERATORS IN THE SMEFT

The primary focus of this paper is the demonstration of  $\gamma_5$  scheme differences in the treatment of four-top operators, since they provide a convenient playground

for investigation due to the factorization of loop integrals. However, considering a complete operator basis in SMEFT, there are other classes of operators that share similar features regarding the treatment of  $\gamma_5$ . Analogous to Sec. IV (but more schematically) we demonstrate in the following that there is also a scheme-dependent finite mixing at one-loop order for operators in the class of  $\psi^2 \phi^2 D$  of Ref. [2].

For the purpose of this discussion, we consider the two operators

$$\begin{aligned} \mathcal{L}_{2t2\phi} &= \frac{\mathcal{C}_{\phi Q}^{(1)}}{\Lambda^2} \bar{Q}_L \gamma_\mu Q_L (\phi^\dagger i \overleftrightarrow{D}^\mu \phi) \\ &+ \frac{\mathcal{C}_{\phi t}}{\Lambda^2} \bar{t}_R \gamma_\mu t_R (\phi^\dagger i \overleftrightarrow{D}^\mu \phi), \end{aligned} \quad (60)$$

where we introduced the short-hand notation

$$i \overleftrightarrow{D}^\mu = i D^\mu - i \overleftarrow{D}^\mu. \quad (61)$$

Similar to the four-top operators in Eq. (2), the operators in Eq. (60) are composed of current-current interactions including chiral vector currents. These current-current operators can be generated by integrating out a new heavy vector particle at tree-level that couples to the SM currents. A concrete and comparably easy realization is given e.g. by the Third Family Hypercharge Model [55, 56]. We restrict the direct evaluation of one-loop contributions of the operators in Eq. (60) to the gaugeless limit of the SM<sup>6</sup> and only investigate the contribution to the chromomagnetic form factor, since this is sufficient to point out the necessity of a more exhaustive study in future work.

An explicit evaluation of the one-loop correction to  $g \rightarrow t\bar{t}$  in the broken phase leads to

$$\begin{aligned} &= \frac{\mathcal{C}_{\phi Q}^{(1)} - \mathcal{C}_{\phi t}}{\mathcal{C}_{tG}} K_{tG}^{2t2\phi} \times g \text{ (diagram) } + \dots \end{aligned} \quad (62)$$

where the gluon and top quarks are taken on-shell<sup>7</sup> and the Gordon identity for on-shell fermions is applied to arrive at this result. The (...) in Eq. (62) represent

<sup>6</sup> In the gaugeless limit, the SM gauge bosons are completely decoupled from the rest of the theory, taking the limit  $g_1 \rightarrow 0$  and  $g_2 \rightarrow 0$ . The Goldstone fields of the SM Higgs doublet are therefore massless physical degrees of freedom. The explicit analytic results in this section are equivalent to the pure Goldstone contribution in Landau gauge.

<sup>7</sup> Even if this choice is not kinematically allowed, it simplifies the extraction of the chromomagnetic contribution.

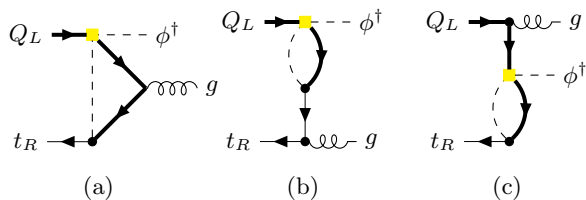


Figure 6: Contribution to the chromomagnetic operator with a single insertion of  $\mathcal{O}_{t\phi}$  (yellow square dot) in the unbroken phase.

contributions to vector and axial form factors that are completely removed using on-shell renormalisation of the external top fields. For the scheme-dependent value of  $K_{tG}^{2t2\phi}$  we find

$$K_{tG}^{2t2\phi} = \frac{g_s m_t}{16\sqrt{2}v\pi^2} \times \begin{cases} 1 & (\text{NDR}) \\ \frac{2}{3} & (\text{BMHV}) . \end{cases} \quad (63)$$

A mapping of  $\mathcal{C}_{tG}$  from one scheme to the other in the presence of the operators of Eq. (60) is therefore achieved considering the difference

$$\Delta K_{tG}^{2t2\phi} = K_{tG}^{2t2\phi, \text{NDR}} - K_{tG}^{2t2\phi, \text{BMHV}} = \frac{g_s m_t}{48\sqrt{2}v\pi^2} , \quad (64)$$

similarly as in Eq. (45).

The same difference is obtained in the unbroken phase, evaluating diagrams of the form of Fig. 6 for both operators. This provides a solid cross check of the scheme-dependent nature which even holds when the SM gauge bosons are part of the theory, since they cannot contribute to the chromomagnetic operator at one-loop order.

The result of Eq. (62) (and the analogous calculation in the unbroken phase) illustrates well that we observe a scheme-dependent finite mixing at one-loop between the operators of Eq. (60) and other operators, just like in the case of four-top operators. Similarly to Sec. VI a map of finite scheme-dependent shifts in the Wilson coefficients could be verified by an explicit on-shell one-loop matching with an adequate toy model.

Regarding the contribution of those operators to the Higgs-gluon coupling, we refrain from performing the complete calculation as in Sec. V in our current work. Even in the simplified scenario of the gaugeless limit, the contributions of the operators would lead to genuine two-loop Feynman integrals, which is beyond the scope of what we would like to demonstrate here. With the observed scheme dependence at one-loop, we already expect a  $\gamma_5$  scheme dependence for the single pole in  $gg \rightarrow h$  and for the RGE of  $\mathcal{C}_{\phi G}$ . As in the case of four-top operators, it should be resolved considering the map of finite shifts in the Wilson coefficients derived at one-loop. However, it is not guaranteed that the renormalised amplitude of the  $gg \rightarrow h$  would have a scheme-independent form once such shifts are considered. On the contrary, it may be

necessary to identify finite scheme-dependent shifts appearing at the two-loop level.

## VIII. CONCLUSIONS

We have computed the contribution of four-top operators to the Higgs-gluon coupling at two-loop level in the SMEFT. We have discussed in detail, for the first time for this process, the differences between the two schemes for the continuation of  $\gamma_5$  to  $D$  space-time dimensions considered in this paper, namely NDR and BMHV. This process is an interesting show-case for the topic of scheme-dependence, because it shows some key features of two-loop computations without adding too many difficulties with respect to a one-loop computation.

Although the results at two-loop level in the two  $\gamma_5$  schemes have a different form, this difference can be accounted for by allowing that the parameters have different values in the two schemes. Given this, we determined in Eqs. (45-47) a mapping between the parameters in the two schemes that makes both the anomalous dimension matrix and the finite result scheme-independent. This extends the approach presented in Ref. [48], where the scheme-independence of the anomalous dimension matrix only is discussed.

We validated the relations between the parameters in the different schemes using some UV models, as detailed in Sec. VI. These simplified UV models support the expectation that the physical result does not depend on the scheme used for  $\gamma_5$ , if such scheme is used consistently. However, we remark that this holds for a top-down approach, in which the EFT (in this case, the SMEFT) is used as an intermediate step.

In the context of the SMEFT with a new physics scale  $\Lambda \sim 1$  TeV, the finite terms in the matrix element can be of the same size as the logarithmically enhanced contributions, and thus can be phenomenologically relevant [8]. For this reason, deriving a connection between the two schemes is very desirable in the perspective of a global fit, where the observables may be computed in different schemes. To this aim, Eqs. (45-47) represent a first effort in the direction of a comprehensive map between the two schemes. We remark that the continuation scheme for  $\gamma_5$  is only one of the calculational choices that could affect the interpretation of SMEFT fits from a bottom-up point of view (see e.g. Refs. [57-59]).

Lastly, we have observed that the interplay of four-top and other SMEFT operators cannot be fully understood in terms of the canonical SMEFT power counting, as in some cases operators that are expected to contribute to different orders based on this counting cannot be treated independently. When the canonical power counting is supplemented by a loop counting like the one discussed in Ref. [21], the observed interplay is more naturally accounted for, under the generic assumption of weakly-coupled and renormalisable UV theories. Furthermore, when the loop counting is considered, the shifts

we have presented can be of the same order of magnitude as the Wilson coefficients themselves (see Eq. (45)). As a consequence, experimental constraints on the determination of Wilson coefficients of loop-generated operators (like  $\mathcal{C}_{tG}$  in this paper) could be interpreted as suffering from large uncertainties, if scheme-dependent contributions from tree-level-generated chiral operators entering at higher explicit loop orders are omitted (in our case, four-top and  $\psi^2\phi^2D$  operators). This points to the necessity of selecting operators contributing to a physical process such that loop counting and canonical-dimension counting are combined, even though it implies assumptions on the UV completion. In any case, a detailed documentation of continuation and renormalisation scheme choices used in EFT calculations and fits of Wilson coefficients is highly recommended.

## ACKNOWLEDGMENTS

We are indebted to Luca Silvestrini, whose comments and suggestions were crucial during the early stages of this project. We would like to thank various people for discussion: Jorge de Blas, Gerhard Buchalla, Hesham El Faham, Ulrich Haisch, Paride Paradisi, Luca Vecchi and Eleni Vryonidou. We also thank Lina Alasfar for providing assistance in automatising parts of the computation. The Feynman diagrams shown in this work were drawn with `TikZ-Feynman` ([60]). This project has received funding from the European Union's Horizon Europe research and innovation programme under the Marie Skłodowska-Curie Staff Exchange grant agreement No 101086085 – ASYMMETRY. The research of GH and JL was supported by the Deutsche Forschungsgemeinschaft (DFG, German Research Foundation) under grant 396021762 - TRR 257. RG and MV acknowledge support from a departmental research grant under the project ‘‘Machine Learning approach to Effective Field Theories in Higgs Physics’’. This work is supported in part by the Italian MUR Departments of Excellence grant 2023-2027 ‘‘Quantum Frontiers’’. SDN also thanks the Lawrence Berkeley National Laboratory, Berkeley Center for Theoretical Physics and the Institute for Theoretical Physics at KIT for hospitality.

## Appendix A: The $h \rightarrow b\bar{b}$ rate

We would like to shortly discuss the computation of the four-quark operators to the  $h \rightarrow b\bar{b}$  rate both in the NDR and BMHV scheme, which we obtain as a side product of our analysis. The operators relevant for our discussion

are

$$\begin{aligned} \mathcal{L}_b = & \frac{\mathcal{C}_{Qb}^{(1)}}{\Lambda^2} (\bar{Q}_L \gamma_\mu Q_L) (\bar{b}_R \gamma^\mu b_R) \\ & + \frac{\mathcal{C}_{Qb}^{(8)}}{\Lambda^2} (\bar{Q}_L T^A \gamma_\mu Q_L) (\bar{b}_R T^A \gamma^\mu b_R) \\ & + \left[ \frac{\mathcal{C}_{QtQb}^{(1)}}{\Lambda^2} (\bar{Q}_L t_R) i\tau_2 (\bar{Q}_L^T b_R) + \text{H.c.} \right] \\ & + \left[ \frac{\mathcal{C}_{QtQb}^{(8)}}{\Lambda^2} (\bar{Q}_L T^A t_R) i\tau_2 (\bar{Q}_L^T T^A b_R) + \text{H.c.} \right] \\ & + \left[ \frac{\mathcal{C}_{b\phi}}{\Lambda^2} (\phi^\dagger \phi) \bar{Q}_L \phi b_R + \text{H.c.} \right]. \end{aligned} \quad (\text{A1})$$

We consider also scalar operators  $\mathcal{O}_{QbQt}^{(1,8)}$  which are neglected in the  $gg \rightarrow h$  computation since they are suppressed by a factor of  $m_b/m_t$ . Including the above operators at NLO, the Higgs decay to bottom quarks is given by [61]<sup>8</sup>

$$\begin{aligned} \frac{\Gamma_{h \rightarrow b\bar{b}}^{\text{NDR}}}{\Gamma_{h \rightarrow b\bar{b}}^{\text{SM}}} = & 1 - \frac{m_t}{m_b} \frac{m_h^2}{32\pi^2\Lambda^2} \left( 7\mathcal{C}_{QtQb}^{(1)} + \frac{4}{3}\mathcal{C}_{QtQb}^{(8)} \right) \\ & \times \left( 2\beta^3 \log\left(\frac{\beta-1}{\beta+1}\right) - 5\beta^2 \right. \\ & \left. + (1-3\beta^2) \log\left(\frac{\tilde{\mu}^2}{m_t^2}\right) + 1 \right) \\ & - \frac{m_h^2}{16\pi^2\Lambda^2} \left( \mathcal{C}_{Qb}^{(1)} + \frac{4}{3}\mathcal{C}_{Qb}^{(8)} \right) \left( 4\beta_b^3 \log\left(\frac{\beta_b-1}{\beta_b+1}\right) \right. \\ & \left. + 7\beta_b^2 + (6\beta_b^2 - 2) \log\left(\frac{\tilde{\mu}^2}{m_b^2}\right) - 1 \right) + \mathcal{O}\left(\frac{1}{\Lambda^4}\right), \end{aligned} \quad (\text{A2})$$

and  $\beta$  defined in Eq. (19) and  $\beta_b$  is obtained from  $\beta$  by replacing  $m_t$  with  $m_b$ . The correct branch of the logarithm can be obtained by  $m_h^2 \rightarrow m_h^2 + i0$ . In the BMHV scheme instead the result of the scalar operators does not change with respect to the NDR scheme, but we obtain a different result for the operators  $\mathcal{C}_{Qb}^{(1)}$  and  $\mathcal{C}_{Qb}^{(8)}$ . We find

$$\frac{\Gamma_{h \rightarrow b\bar{b}}^{\text{NDR}} - \Gamma_{h \rightarrow b\bar{b}}^{\text{BMHV}}}{\Gamma_{h \rightarrow b\bar{b}}^{\text{SM}}} = \frac{\mathcal{C}_{Qb}^{(1)} + \frac{4}{3}\mathcal{C}_{Qb}^{(8)}}{8\pi^2\Lambda^2} (m_h^2 - 6m_b^2) + \mathcal{O}\left(\frac{1}{\Lambda^4}\right). \quad (\text{A3})$$

At tree-level one has  $\Gamma_{h \rightarrow b\bar{b}}^{\text{X,TL}} \propto (g_{h\bar{b}b}^{\text{X}})^2$ , being X=NDR, BMHV, where  $g_{h\bar{b}b}^{\text{X}}$  contains corrections from the operator  $\mathcal{O}_{b\phi}$ , as can be seen from Eq. (7) (replacing  $t$  with  $b$ ). Keeping into account the different value of such coupling in the two regularisation schemes, namely

<sup>8</sup> In this reference, the on-shell renormalisation scheme is employed. For this reason, we perform the check with the bare amplitude, Eqs. (4.13), (4.14).

Eq. (46), we can write

$$\frac{\Gamma_{h \rightarrow b\bar{b}}^{\text{NDR,TL}} - \Gamma_{h \rightarrow b\bar{b}}^{\text{BMHV,TL}}}{\Gamma_{h \rightarrow b\bar{b}}^{\text{SM}}} = \frac{\mathcal{C}_{Qb}^{(1)} + \frac{4}{3}\mathcal{C}_{Qb}^{(8)}}{8\pi^2\Lambda^2} (6m_b^2 - m_h^2) + \mathcal{O}\left(\frac{1}{\Lambda^4}\right). \quad (\text{A4})$$

If one consistently accounts for the orders in the loop expansion and the  $1/\Lambda^2$  expansion, one is then able to obtain a scheme-independent result for this process.

## Appendix B: Renormalisation Group Equations and counterterms

The anomalous dimension matrix of a theory is strictly connected to the structure of the divergences of the theory itself. In this appendix we analyse in detail this relation, deriving a general formula which can be used to determine the one-loop counterterms associated to SMEFT operators by simply reading the corresponding entry of the renormalisation group equation, given for example in [43, 44, 62] (or viceversa).

We present here a general argument where a generic SMEFT operator  $\mathcal{O}_2$  renormalises a different operator  $\mathcal{O}_1$ . We fix, coherently with the rest of the paper,

$$\mathcal{C}_1^{\text{MS}}(\mu) = \mathcal{C}_1^{(0)} + \delta\mathcal{C}_1(\mu), \quad (\text{B1})$$

$$\delta\mathcal{C}_1(\mu) = \frac{A}{\epsilon} Y(\mu)^{N_Y} \lambda(\mu)^{N_\lambda} g(\mu)^{N_g} \mathcal{C}_2(\mu). \quad (\text{B2})$$

In the previous expression,  $\mu$  is the renormalisation scale (on which the MS parameters depend) and  $Y, \lambda, g$  denote, respectively, a Yukawa coupling, the Higgs quartic coupling and a gauge coupling and  $A$  is a number that does not depend on the renormalisation scale (nor implicitly or explicitly).

When dimensional regularisation is used, it is customary to rescale the parameters in such a way they maintain their physical dimension:  $X \rightarrow \mu^{\kappa_X \epsilon} X$ . A typical example is given by gauge couplings, for which  $\kappa_g = 1$  is chosen to keep them dimensionless ( $g \rightarrow \mu^\epsilon g$ ). This operation should be done also for the coefficients of the SMEFT operators, whose mass dimension in  $D$  space-time dimensions is different from  $-2$ .<sup>9</sup> Remarkably, SMEFT operators may have a different dimension depending on their field content, even if in the limit  $D \rightarrow 4$  they all have dimension six. Since the product  $\mathcal{C}_i \mathcal{O}_i$  must have dimension  $D$  one has, in principle, 8 different rescaling factors  $\kappa_i$ , one for each of the operator classes defined in [2]. As we will see at the end of this section, keeping this

aspect into account is crucial in order to find the correct relation between counterterms and anomalous dimension entries.

The renormalisation group equation for  $\mathcal{C}_1$  can be obtained from (dropping the superscript MS for a better readability)

$$0 = \mu \frac{d\mathcal{C}_1^{(0)}(\mu)}{d\mu} = \mu \frac{d}{d\mu} \left( \mu^{\kappa_1 \epsilon} (\mathcal{C}_1(\mu) - \delta\mathcal{C}_1(\mu)) \right). \quad (\text{B3})$$

Since in the end we will take  $D \rightarrow 4$ , we need the first term of the expansion in the  $\beta$ -function for each of the parameters contained in the counterterm, namely

$$\mu \frac{dX(\mu)}{d\mu} \equiv \beta_X = -\kappa_X \epsilon + \mathcal{O}(1). \quad (\text{B4})$$

Performing the algebra in Eq. (B3) and using Eq. (B4) we obtain

$$\begin{aligned} \mu \frac{d\mathcal{C}_1(\mu)}{d\mu} &= A \times (\kappa_1 - \kappa_2 - N_Y - N_g - 2N_\lambda) \\ &\times Y(\mu)^{N_Y} \lambda(\mu)^{N_\lambda} g(\mu)^{N_g} \mathcal{C}_2(\mu). \end{aligned} \quad (\text{B5})$$

If we normalise the anomalous dimension matrix as

$$\mu \frac{d\mathcal{C}_1(\mu)}{d\mu} = \frac{1}{16\pi^2} \gamma_{12}(\mu) \mathcal{C}_2(\mu), \quad (\text{B6})$$

we can write (comparing this expression with Eq. (B2))

$$\delta\mathcal{C}_1(\mu) = \frac{1}{16\pi^2 \epsilon} \gamma_{12}(\mu) \mathcal{C}_2(\mu) \frac{1}{\kappa_1 - \kappa_2 - N_Y - N_g - 2N_\lambda}. \quad (\text{B7})$$

A practical example of this formula is Eq. (33). Four-top operators  $\mathcal{O}_{Q_t}^{(1,8)}$  renormalise  $\mathcal{O}_{t\phi}$  at  $\mathcal{O}(Y_t \lambda)$  [43] and at  $\mathcal{O}(Y_t^3)$  [44]. This means  $(N_Y, N_g, N_\lambda) = (1, 0, 1)$  ( $(3, 0, 0)$ ) for the former (latter) case.

In  $D = 4 - 2\epsilon$  space-time dimensions one has

$$\dim[\mathcal{C}_{Q_t}^{(1,8)}] = 2\epsilon, \quad \dim[\mathcal{C}_{t\phi}] = 3\epsilon, \quad (\text{B8})$$

which implies  $\kappa_{Q_t} = 2$ ,  $\kappa_{t\phi} = 3$ .

Plugging these numbers in Eq. (B7) gives Eq. (33) (for both terms of  $\mathcal{O}(Y_t \lambda)$ ,  $\mathcal{O}(Y_t^3)$ ).

## Appendix C: Additional results

We present in this appendix  $\mathcal{A}_{g_{h\bar{t}t} + m_t}$  introduced in Eq. (39)

<sup>9</sup> Within the notation used in this paper, the coefficients are written as  $\mathcal{C}_i/\Lambda^2$ , being  $\mathcal{C}_i$  a dimensionless quantity.



- [22] C. Arzt, M. B. Einhorn, and J. Wudka, *Nucl. Phys. B* **433**, 41 (1995), [arXiv:hep-ph/9405214](#).
- [23] G. F. Giudice, C. Grojean, A. Pomarol, and R. Rattazzi, *JHEP* **06**, 045 (2007), [arXiv:hep-ph/0703164](#).
- [24] R. Contino, M. Ghezzi, C. Grojean, M. Muhlleitner, and M. Spira, *JHEP* **07**, 035 (2013), [arXiv:1303.3876 \[hep-ph\]](#).
- [25] G. Buchalla, O. Cata, and C. Krause, *Nucl. Phys. B* **894**, 602 (2015), [arXiv:1412.6356 \[hep-ph\]](#).
- [26] C. Englert, P. Galler, and C. D. White, *Phys. Rev. D* **101**, 035035 (2020), [arXiv:1908.05588 \[hep-ph\]](#).
- [27] C. Müller, *Phys. Rev. D* **104**, 095003 (2021), [arXiv:2102.05040 \[hep-ph\]](#).
- [28] G. Buchalla, M. Höfer, and C. Müller-Salditt, *Phys. Rev. D* **107**, 076021 (2023), [arXiv:2212.08560 \[hep-ph\]](#).
- [29] G. Guedes, P. Olgoso, and J. Santiago, (2023), [arXiv:2303.16965 \[hep-ph\]](#).
- [30] S. Weinberg, *Phys. Rev. Lett.* **43**, 1566 (1979).
- [31] E. E. Jenkins, A. V. Manohar, and P. Stoffer, *JHEP* **03**, 016 (2018), [arXiv:1709.04486 \[hep-ph\]](#).
- [32] F. Jegerlehner, *Eur. Phys. J. C* **18**, 673 (2001), [arXiv:hep-th/0005255](#).
- [33] J. G. Korner, D. Kreimer, and K. Schilcher, *Z. Phys. C* **54**, 503 (1992).
- [34] D. Kreimer, (1993), [arXiv:hep-ph/9401354](#).
- [35] L. Chen, (2023), [arXiv:2304.13814 \[hep-ph\]](#).
- [36] M. Ciuchini, E. Franco, G. Martinelli, and L. Reina, *Nucl. Phys. B* **415**, 403 (1994), [arXiv:hep-ph/9304257](#).
- [37] H. Béliusca-Maïto, A. Ilakovac, P. Kühler, M. Mađor-Božinović, D. Stöckinger, and M. Weißwange, *Symmetry* **15**, 622 (2023), [arXiv:2303.09120 \[hep-ph\]](#).
- [38] C. Cornella, F. Feruglio, and L. Vecchi, *JHEP* **02**, 244 (2023), [arXiv:2205.10381 \[hep-ph\]](#).
- [39] P. Nogueira, *J. Comput. Phys.* **105**, 279 (1993).
- [40] R. Mertig, M. Bohm, and A. Denner, *Comput. Phys. Commun.* **64**, 345 (1991).
- [41] V. Shtabovenko, R. Mertig, and F. Orellana, *Comput. Phys. Commun.* **207**, 432 (2016), [arXiv:1601.01167 \[hep-ph\]](#).
- [42] V. Shtabovenko, R. Mertig, and F. Orellana, *Comput. Phys. Commun.* **256**, 107478 (2020), [arXiv:2001.04407 \[hep-ph\]](#).
- [43] E. E. Jenkins, A. V. Manohar, and M. Trott, *JHEP* **10**, 087 (2013), [arXiv:1308.2627v4 \[hep-ph\]](#).
- [44] E. E. Jenkins, A. V. Manohar, and M. Trott, *JHEP* **01**, 035 (2014), [arXiv:1310.4838v3 \[hep-ph\]](#).
- [45] M. Grazzini, A. Ilnicka, and M. Spira, *Eur. Phys. J. C* **78**, 808 (2018), [arXiv:1806.08832 \[hep-ph\]](#).
- [46] N. Deuschmann, C. Duhr, F. Maltoni, and E. Vryonidou, *JHEP* **12**, 063 (2017), [Erratum: *JHEP* **02**, 159 (2018)], [arXiv:1708.00460 \[hep-ph\]](#).
- [47] M. Ciuchini, E. Franco, L. Reina, and L. Silvestrini, *Nucl. Phys. B* **421**, 41 (1994), [arXiv:hep-ph/9311357](#).
- [48] M. Ciuchini, E. Franco, G. Martinelli, L. Reina, and L. Silvestrini, *Phys. Lett. B* **316**, 127 (1993), [arXiv:hep-ph/9307364](#).
- [49] A. J. Buras, M. Misiak, M. Munz, and S. Pokorski, *Nucl. Phys. B* **424**, 374 (1994), [arXiv:hep-ph/9311345](#).
- [50] S. Herrlich and U. Nierste, *Nucl. Phys. B* **455**, 39 (1995), [arXiv:hep-ph/9412375](#).
- [51] M. J. Dugan and B. Grinstein, *Phys. Lett. B* **256**, 239 (1991).
- [52] J. de Blas, J. C. Criado, M. Perez-Victoria, and J. Santiago, *JHEP* **03**, 109 (2018), [arXiv:1711.10391 \[hep-ph\]](#).
- [53] J. Fuentes-Martín, M. König, J. Pagès, A. E. Thomsen, and F. Wilsch, *JHEP* **02**, 031 (2023), [arXiv:2211.09144 \[hep-ph\]](#).
- [54] A. Dedes, W. Materkowska, M. Paraskevas, J. Rosiek, and K. Suxho, *JHEP* **06**, 143 (2017), [arXiv:1704.03888 \[hep-ph\]](#).
- [55] B. C. Allanach and J. Davighi, *JHEP* **12**, 075 (2018), [arXiv:1809.01158 \[hep-ph\]](#).
- [56] B. C. Allanach and H. Banks, *Eur. Phys. J. C* **82**, 279 (2022), [arXiv:2111.06691 \[hep-ph\]](#).
- [57] T. Corbett, A. Martin, and M. Trott, *JHEP* **12**, 147 (2021), [arXiv:2107.07470 \[hep-ph\]](#).
- [58] A. Martin and M. Trott, (2023), [arXiv:2305.05879 \[hep-ph\]](#).
- [59] J. Aebischer, M. Pesut, and Z. Polonsky, (2023), [arXiv:2306.16449 \[hep-ph\]](#).
- [60] J. Ellis, *Comput. Phys. Commun.* **210**, 103 (2017), [arXiv:1601.05437 \[hep-ph\]](#).
- [61] R. Gauld, B. D. Pecjak, and D. J. Scott, *JHEP* **05**, 080 (2016), [arXiv:1512.02508 \[hep-ph\]](#).
- [62] R. Alonso, E. E. Jenkins, A. V. Manohar, and M. Trott, *JHEP* **04**, 159 (2014), [arXiv:1312.2014v4 \[hep-ph\]](#).